J Mol Model (2012) 18:4113–4120
DOI 10.1007/s00894-012-1413-4

ORIGINAL PAPER

DFT study of the interaction between the conjugated fluorescein and dabcyl system, using fluorescene quenching method

Mónica Alvarado-González · Marco Gallo · Pablo Lopez-Albarran · Norma Flores-Holguín · Daniel Glossman-Mitnik

Received: 1 February 2012 / Accepted: 22 March 2012 / Published online: 17 April 2012

Abstract Molecular beacon is a DNA probe containing a sequence complementary to the target that is flanked by self-complementary termini, and carries a fluorophore and a quencher at the ends. We used the fluorescein and dabcyl as fluorophore and quencher respectively, and studied with DFT calculations at the GGA/DNP level, and taking into account DFT dispersion corrections by the Grimme and Tkatchenko-Scheffler (TS) schemes, the distance, where the most favorable energetic interaction between the fluorophore and quencher in conjugated form occurs. This distance occurs at a separation distance of 29.451 Å between the centers of Dabcyl and fluorescein employing the TS DFT dispersion correction scheme, indicating FRET efficiency around 94.28 %. The calculated emission spectra of the conjugated pair in water indicated that the emission and absorption spectrum overlap completely and thus no fluorescence can be observed due to the fluorescence resonance energy transfer (FRET) effect. The DFT results confirmed the experimentally observing fluorescence quenching of the fluorescein-dabcyl conjugated system by FRET.

Keywords Dabcyl · DFT · Fluorescein · FRET · Interaction energy · Molecular beacons

M. Alvarado-González (✉)
Centro de Investigación en Alimentación y Desarrollo (CIAD),
A. C. Av. Cuarta sur No. 3820, Fracc. Vencedores del Desierto.,
33089 Unidad Delicias, Chihuahua, Mexico
e-mail: salvarado@ciad.mx

M. Gallo
Facultad de Ciencias Químicas, Universidad Autónoma de San Luis Potosí,
Av. Manuel Nava No. 6, Zona Universitaria,
San Luis Potosí, SLP 78210, Mexico

P. Lopez-Albarran
Facultad de Ingeniería en Tecnología de la Madera, Universidad Michoacana de San Nicolás de Hidalgo,
Av. Fco. J. Muciga S/N,
58030 Morelia, Michoacan, Mexico

N. Flores-Holguín · D. Glossman-Mitnik
Laboratorio Virtual NANOCOSMOS, CIMAV,
Miguel de Cervantes 120, Complejo Industrial Chihuahua,
Chihuahua, Chih 31109, Mexico

Introduction

The molecular beacon (MB) principle is based on hybridization, that is these molecular probes experience spontaneous conformational changes when the single stranded nucleic acid molecules in the loop hybridize to a complementary nucleic acid sequence in their target, resulting in the emission of fluorescence [1].

Molecular beacons are probes having single stranded nucleic acid molecules with a stem and loop structure. The loop portion of the molecule contains a sequence that is complementary to a predetermined sequence in a target nucleic acid. The stem is formed by the annealing of two complementary arm sequences that are on either side of the probe sequence, the arm sequences in the probe are unrelated to the target sequence. A fluorophore is covalently attached to one end of the arm, and a nonfluorescent quencher is covalently attached to the end of the other arm. In the absence of a target, the stem of the hairpin holds the fluorophore so close to the quencher that fluorescence does not occur. When the probe encounters a target molecule it forms a hybrid that is more stable and longer than the hybrid formed by the arm sequences, the probe binds to its target causing a conformational change that forces the arm sequences to be apart causing the

separation of the fluorophore and the quencher and the restoration of fluorescence. This permits the detection of probe-target hybrids in the presence of unhybridized probes [1, 2].

Molecular beacons are hybridization probes that can report the presence of a complementary nucleic acid targets without having to separate probe-target hybrids from excess probes in hybridization assays [1, 2]. The MB have been developed since 1996, by Tyagi and Kramer [2].

The fundamental mechanism of fluorescence resonance energy transfer (FRET), involves a donor fluorophore in an excited electronic state that transfers its excitation energy to a nearby acceptor (forming a nonfluorescent conjugated system) in a non-radiative fashion through long-range dipole-dipole interactions.

FRET occurs between two appropriately positioned fluorophores only when the distance separating them is 8 to 10 nanometers or less. In the presence of a suitable acceptor, the donor fluorophore can transfer excited state energy directly to the acceptor without emitting a photon [3–5].

Non-radiative energy transfer occurs over much longer distances than short-range solvent effects, and the dielectric nature of constituents solvent positioned between the conjugated system has very little influence on the efficacy of resonance energy transfer, that depends mainly on the distance between the donor and acceptor fluorophore [3–5].

The Förster theory shows that FRET efficiency (Ef_{FRET}) varies as the inverse sixth power of the distance between the two geometrical molecules centers (R) [3–5]:

$$Efret = \frac{Ro^6}{Ro^6 + R^6}, \tag{1}$$

where Ro is the characteristic distance where the FRET efficiency is 50 percent, which can be calculated for any pair of fluorescent molecules (also termed the Förster radius). For distances less than Ro, the FRET efficiency is close to maximal, whereas for distances greater than Ro, the efficiency rapidly approaches zero.

$$Ro = \left(8.8x10^{23} JK^2 Qo\, n^{-4}\right)^{1/6}, \tag{2}$$

where K^2 is the orientation factor for a dipole–dipole interaction, J is the spectral overlap integral (the region of overlap between the two spectra), Qo is the quantum yield of donor without acceptor, and n is the refractive index of the medium between the donor and acceptor. Most of the parameters in Eq. 2 are constants that are obtained from the literature [3–5].

For Fluorescein and dabcyl the forster radius Ro corresponds to the value of 46.97 Å. It is important to notice that the level of a FRET signal can be reduced if the two fluorophores are not properly aligned (K^2 value of approximately zero) or if they are simply not positioned within the Förster radius [3–5].

If the fluorescence is inhibited this signals that the acceptor and donor molecules are within the Foster radius. It is important to stress that when fluorescein in the conjugated system fluoresce at its individual characteristic emission wave length, this indicates that the distance between donor and acceptor surpass the foster radius [3–5] and FRET has not been observed.

Currently the requirements for high-sensitivity and high-affinity of molecular biological probe are becoming increasingly urgent. In this area the MB have been applied for real-time monitoring of polymerase chain reactions [1, 6], developing DNA sensors [7], analysis in vivo [6], drug developing [8]. In recent years, the structure of MBs has presented many improvements. MBs technology not only shares a wide range of applications in the study of biology, but also will play an important role in the detection and diagnosis of genetic diseases, basic and clinical biomedical research.

Melting temperature [9, 10], the chain length of stem, the GC nucleotide content, the ionic concentration [10] and the distance and alignment between fluorophore and quencher in conjugated form [1, 11] are the most important factors, that determine the correct function of MB. The Fluorophore-quencher conjugated system is in charge of signaling the hybridization of the probe with the DNA target, by the appearance of fluorescence.

In this work we studied the spectrum and the energetic interaction between the fluorophore-quencher conjugated, described by fluorescein-dabcyl molecules to obtain molecular level information that is difficult to get experimentally, such as the most stable geometrical conformation for the conjugated system (most favorable interaction energy), the separation distance between the fluorescein-dabcyl molecules at the most stable conformation and the FRET efficiency (fluorescence signal) for this geometrical conformation.

The molecular level information obtained in this work by applying theoretical tools of computational chemistry, using DFT calculations that include dispersion corrections, can help scientists design other MB systems with strong fluorescence signal with special significance in molecular diagnosis and in the development of DNA sensors.

Computational methods

The fluorescein and dabcyl, models studied were obtained from the libraries of the National Center for Biotechnology Information (NCBI). All computational DFT studies were performed with the Material Studio 5.5 and the GAUSSIAN03W programs [12, 13].

In this work we used density functional theory (DFT), with the PBE1PBE hybrid functional by Perdue, Burke and Ernzerhof, which uses 25 % HF exchange and 75 % correlation weighting functional [14–16].

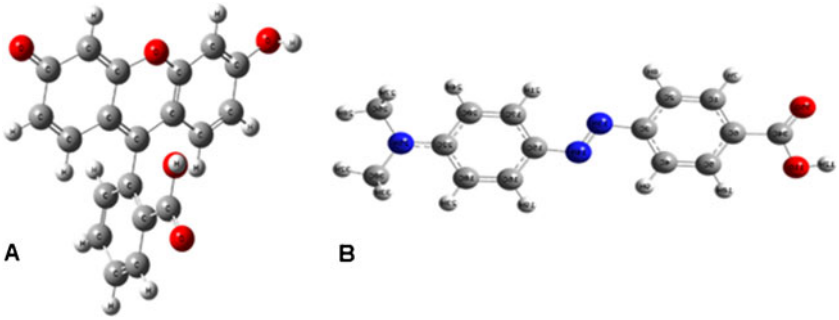

Fig. 1 Optimized geometries of fluorescein (**a**), and dabcyl (**b**). Carbon atoms are in gray color, oxygen atoms are in red, nitrogen atoms in blue, and hydrogen atoms are in white color

The ground state geometry of both molecules were optimized using GGA/PBE 6-31G (d,p) basis sets [13], from this calculations we obtained, the highest occupied molecular orbital HOMO) and the lowest unoccupied molecular orbital (LUMO) distributions. The optimized geometries for dabcyl and fluorescein are shown in Fig. 1.

Initially we placed the fluorescein and dabcyl at six different positions, with a separation distance between 25–35 Å that corresponds to FRET efficiencies between 97.48 % and 84.92 %. The efficiencies were calculated according to Eqs. 1 and 2 and the constants described by Kim et al. [5]. Molecular beacons are capable of spanning a large conformational space, mediated by the multiple rotameric states of the aliphatic thiol linker of the fluorophore and the linker of dabcyl [5]. Since the donor and acceptors are attached at the ends of the stem formed by the annealing of two complementary sequences situated on either side of the probe sequence (arms), the only conformations permitted to the acceptor and donors, due to the rigidity of the arms are turns, that is why in our conjugated systems we only specified turns of the molecules as shown in Fig. 2 and calculated their interaction energy at these conformations.

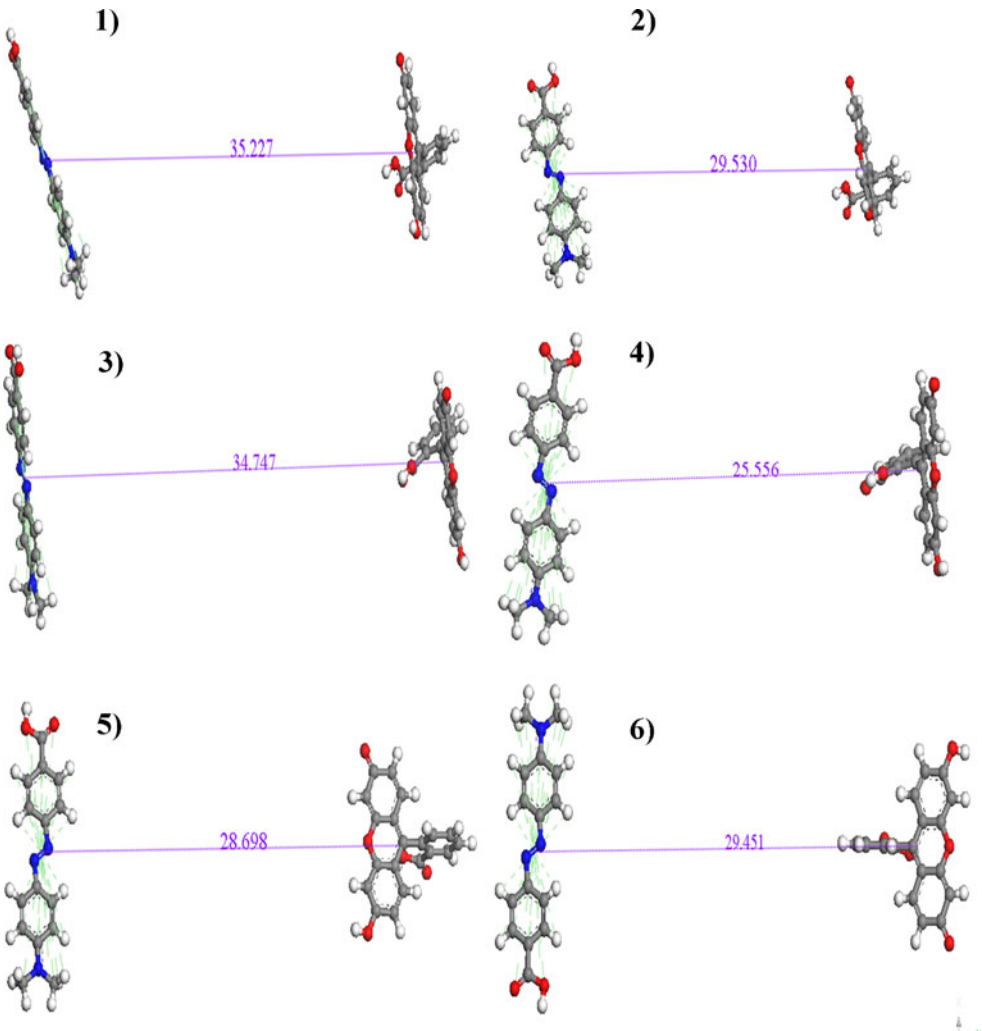

Fig. 2 Optimized geometries for six different conjugated systems, created by allowing different rotameric states. Carbon atoms are in gray color, oxygen atoms are in red, nitrogen atoms in blue, and hydrogen atoms are in white color

It is also important to note that since dabcyl is a neutral and hydrophobic molecule, there is neither attraction or repelling between both molecules without affecting the stability of the stem hybrid [1]. Also due to this neutral nature of dabcyl, and the large distances of separation between fluorophore and dabcyl, the energetic influence on the conjugated system by the nucleotides near the fluorophore and quencher is minimal, therefore those nucleotides are not included in our models.

The following analysis was carried for each conjugated system:

First we carried a ground state geometry optimization at the GGA-PBE/DNP level, where DNP stands for double numerical plus polarization basis sets (comparable to a. 6-31G(d,p) basis sets) for the individual donor and acceptor, and then we calculated the geometrical optimization for the conjugated systems at the same level of theory but including DFT dispersion corrections [12] using two schemes that introduce damped atom-pairwise dispersion corrections that were develop by Grimme [17] and by Tkatchenko and Scheffler [18].

It is known that the correct long-range interaction tail, for separated molecules, is absent from all popular local-density or gradient corrected exchange-correlation functionals of density-functional theory as well as from the Hartree-Fock (HF) approximation [19, 20].

A popular remedy for the missing vdW interaction in DFT consists of adding a pairwise interatomic C_6R^{-6} term to the DFT energy, that includes a damping function to avoid singularities of the radius at short ranges [17, 18].

At short range, the long-range expression is matched to the DFT potential by multiplication with a damping function $f(R_{ij}^{0},R_{ij})$, which reduces the additional dispersion contribution to zero, subject to a cutoff defined by some suitably calculated combination R_{ij}^{0} of the van der Waals radii of the atom pair. The dispersion-corrected exchange-correlation functional is then formed by simply adding the correction potential to the ordinary DFT exchange-correlation functional. As $C_{6,ij}$ coefficients are additive, the dispersion-corrected total energy E_{tot} may therefore be written as [12, 17, 18]:

$$E_{tot} = E_{DFT} + s_i \sum_{i=1}^{N} \sum_{j>i}^{N} f\left(S_R R_{ij}^{\circ} R_{ij}\right) C_{6,ij} R_{ij}^{-6}, \quad (3)$$

where E_{DFT} is the standard DFT total energy and the sums go over all N atoms in the system.

In existing schemes, the R_{ij}^{0} and $C_{6,ij}$ coefficients are approximated from semiempirically determined parameters. Differences between DFT exchange-correlation functionals in the description of short to medium-range dispersion interaction are taken into account by a suitable modification of the correction potential through the parameters s_6 or S_R.

A serious shortcoming of the C_6R^{-6} schemes is their empirical nature, since the parameters do not depend on the electronic structure, but are rather obtained by fitting to experimental C_6 coefiicients and using training sets, such as the Grimme scheme [17] that neglects the different atomic environments.

The state of the art in the semiempirical correction methods is represented by the Tkatchenko-Scheffler (TS) scheme [18]. This scheme relies on a parameter-free method for an accurate determination of long-range van der Waals interactions from mean-field electronic structure calculations. Their method relies on the summation of interatomic C_6 coefficients, derived from the electron density of a molecule or solid and accurate reference data for the free atoms. They show that the effective atomic *C6* coefficients depend strongly on the bonding environment of an atom in a molecule [18].

Table 1 Distances and FRET efficiencies for the conjugated systems shown in Fig. 2

Conjugated System	Distance (Å)	FRET efficiency
1	35.22	84.92 %
2	29.532	94.19 %
3	34.742	85.94 %
4	25.55	97.48 %
5	28.7	95.06 %
6	29.45	94.28 %

Table 2 Interaction energies for the conjugated systems shown in Fig. 2

	Grimme (kcal/mol)	TS (kcal/mol)
Conjugate 1	−40.33627852	−21.11090878
Conjugate 2	−40.28833683	−19.5468426
Conjugate 3	−40.31017415	−21.62195211
Conjugate 4	−40.32906217	−19.88243441
Conjugate 5	−40.25495335	−22.79589595
Conjugate 6	−40.14011921	−22.99167876

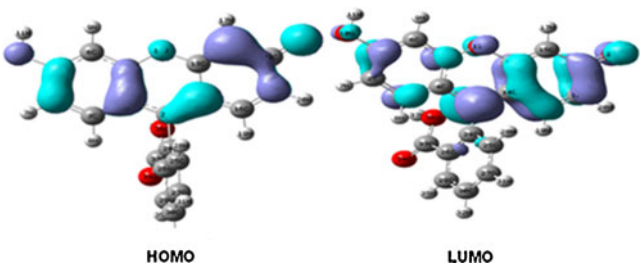

Fig. 3 Frontier molecular orbitals, HOMO and LUMO for fluorescein

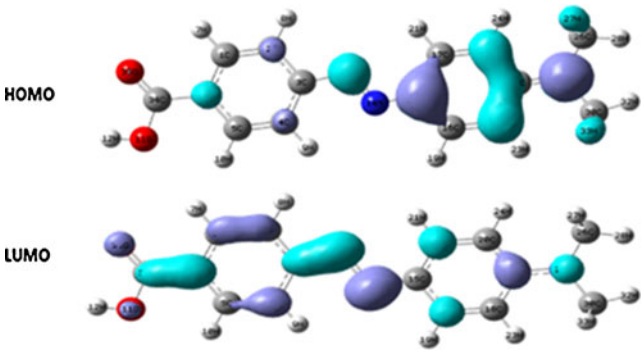

Fig. 4 Frontier molecular orbitals, HOMO and LUMO for Dabcyl

The computed interaction energy was calculated using the following equation.

$$E_{\text{interaction}} = E_{\text{conjugated system}} - E_{\text{fluorescein}} - E_{\text{dabcyl}} \quad (4)$$

The distance between the fluorescein and dabcyl was based on their geometrical centers as defined in the calculation of the forster radius.

In order to asses that fluorescence is quenched within the conjugated system we calculated the fluorescence and absorption spectra using the following methodology employing the GAUSSIAN 03 package for a conjugated system [13, 16].

For the fluorescence spectra the geometry optimization of the first excited state was calculated using TD-DFT, CIS/STO 3G (d), and then the energy, the first excited state was calculated using TD-DFT,6–31 + G(d,p), all calculations were in the presence of water using the IEFPCM solvent model [16].

For the absorption spectra, the geometry optimization of the ground state was calculated at the GGA/PBE level using 6–31G (d,p) basis sets and the energy calculation of the first excited states was calculated using TD-DFT, 6–31 + G(d,p) all calculations were in the presence of water using the IEFPCM polarizable continuum solvent model [16, 21].

The absorption and emission spectra data was processed with the SWizard program [22] (SWizard is a user-friendly program for post processing of spectral data. A spectrum is convoluted as a sum of Gaussian, Lorentzian, or pseudo-Voigt functions), and then visualized using the Origin Pro 7 program [23].

Results and discussion

The interaction energy for the six conjugated systems along with their separation distance and FRET efficiencies are presented in Tables 1 and 2, and the geometric conformations of the six conjugated systems are shown in Fig. 2.

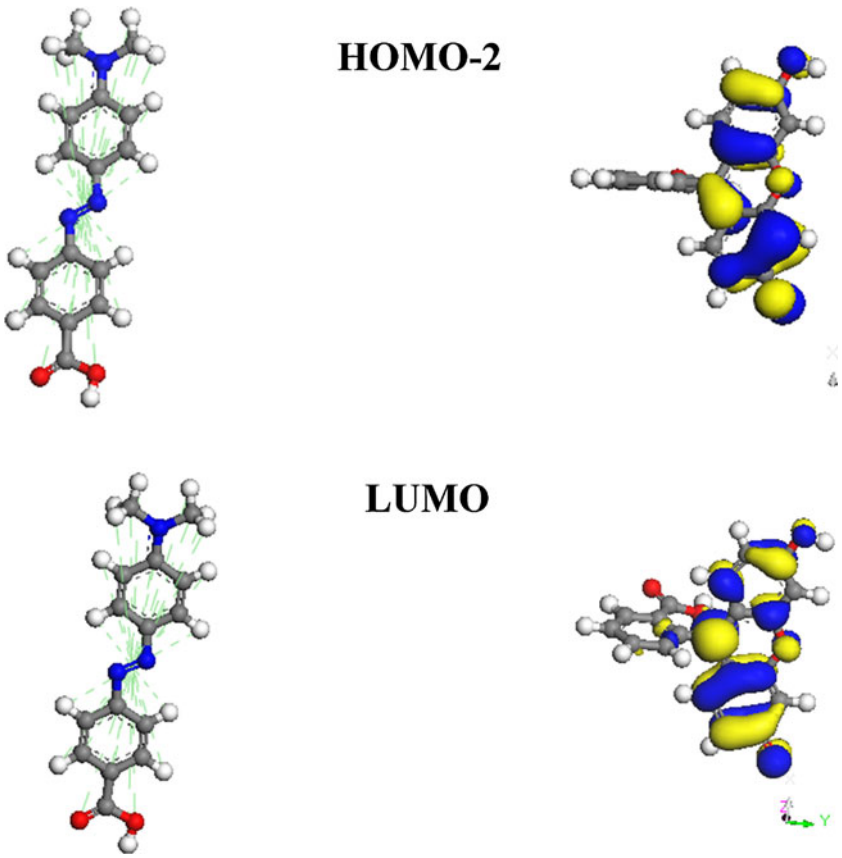

Fig. 5 Molecular orbitals involved in the fluorescence spectra in conjugated 6 TS

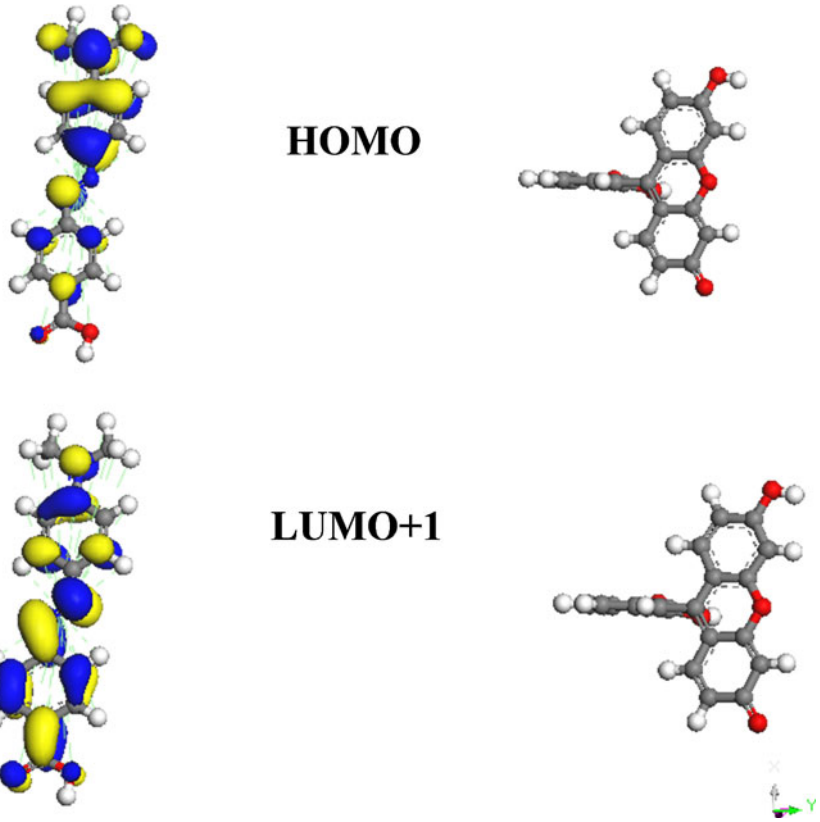

Fig. 6 Molecular orbitals involved in the absorption spectra in conjugated 6 TS

Table 2 shows the interaction energy for the six conjugated conformations employing two different DFT-Dispersion correction schemes. It is interesting to note that the interaction energies for the Grimme scheme are almost twice in value of those interaction energies calculated by the TS scheme.

It is important to highlight that FRET signals the radiationless transfer of excitation energy from donor to acceptor, the efficiency of this energy transfer is usually distance dependent, the shorter the distance between donor to acceptor the higher the FRET efficiency. On the other hand the interaction energy indicates the most stable conformation for the donor and acceptor in a neutral electronic state (no excitations), the more negative the interaction energy the more probable it is that the donor and acceptor are found at this geometrical conformation, since this geometrical conformation has the highest stability it is important to know the FRET efficiency of this conformation in order to evaluate its degree of fluorescence quenching.

The calculations using the Grimme scheme for dispersion corrections [17] showed conjugated 1 as the one having the most favorable interaction energy, even though conjugated 1 has the lowest FRET efficiency from all six conjugated systems, also the interaction energies using the Grimme scheme for all six conjugated system are unrealistic varying around ±0.2 kcal mol^{-1} even though the distances between donor and acceptor have large distance variations from 25–35 Å.

On the other hand the calculations using the TS scheme for dispersion corrections [18] showed that conjugated systems 5 and 6 have the best interaction energy (higher stability) and at the same time very good FRET efficiencies 95.06, 94.28 %. Conjugated systems 2 and 4 have less favorable interaction energies (lower stability, lower probability of

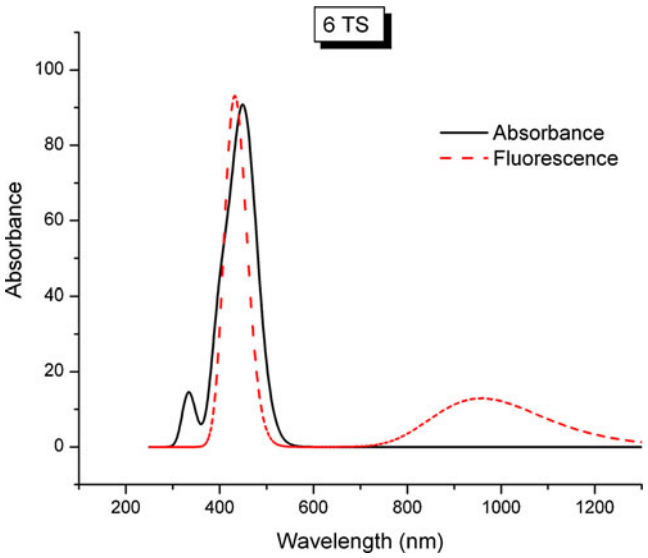

Fig. 7 Theoretical spectra for conjugated 6 TS, the absorption spectra is shown with a black line ——, and the emission spectra is shown with a red dotted line - - - - -

existence), but their FRET efficiencies are very good 94.19 and 97.48 %. In the TS scheme the interaction energies between the six conjugated systems varies around ±2 kcal mol^{-1}, higher energetic variations than in the Grimme scheme.

From Fig. 2 we can observe that the N=N group in dabcyl is closer to the three benzene rings from fluorescein in conjugated 5 than in the conjugated 6 system, since the fluorescein in conjugated 5 is rotated 180 degrees with respect to conjugated 6.

Because the Grimme scheme is a parameterized DFT-dispersion method [17] that relies heavily on a training set, and does not takes the effect of the atomic environment in their dispersion coefficient calculations, in contrast to the TS scheme [18], the results obtained by the TS scheme are more reliable than the results derived from the Grimme scheme.

The frontier orbital of the molecules play an important role in electronic transitions responsible for the emission and absorption spectrum, those orbitals for the individual acceptor and donor are shown in Figs. 3 and 4.

From Fig. 3 and 4, it can be seen that the HOMO and LUMO of fluorescein are mainly localized in the three benzene rings. The HOMO of dabcyl is localized on the benzene ring near the amine group, and the LUMO is localized on the benzene ring near the carboxyl group.

Our calculations shown in Fig. 5 and in Fig. 6 showed the orbitals involved in the fluorescence and absorption spectra of the conjugated 6 using the TS dispersion correction scheme. From Fig. 5 we can observe that the orbitals involved in the fluorescence spectra correspond to the HOMO-2 and LUMO orbitals of the conjugated 6 TS, and these orbitals are located on the fluorescein molecule only. The LUMO orbital density is located mostly on the three benzene rings with very small density on the benzene perpendicular to the three benzene rings. The HOMO-2 orbital lies completely on the three benzene rings with no density on the perpendicular benzene ring.

The calculations in Fig. 6, show that the orbitals involved in the absorption spectra correspond to the HOMO and LUMO+1 orbitals of the conjugated 6 TS, and these orbitals lie only on the dabcyl molecule. The HOMO orbital has scarce density on the carbonyl group of dabcyl similar to the HOMO orbital of the individual molecule. On the other hand the LUMO+1 orbital has good density on the carbonyl group and it is distributed in similar form to the LUMO orbital of the individual dabcyl molecule.

The absorption and fluorescence spectra of conjugated 6 TS that has 94.28 % fret efficiency is shown in Fig. 7, from this figure we can observe two features, first there is a complete overlap between the absorption and fluorescence spectra, and second the fluorescence of fluorescein in the conjugated system is at a wavelength of 432.9 nm, 39.2 nm larger than in the individual molecule [24], from these two features we are certain that quenching of the fluoresce has taken place, in agreement with the experimental results obtained by Tyagi and Kramer [1].

Conclusions

In this article, the interaction energy between fluorescein and dabcyl (fluorescence quenching chromophore) molecules was studied by computational modeling and DFT calculations that include dispersion corrections. The theoretical calculations of the interaction between fluorescein and dabcyl showed the geometrical conformation of fluorescein and dabcyl molecules at the most favorable interaction energy using the DFT with dispersion corrections from the TS scheme (conjugated **6**), which occurs at a distance of 29.45 Å between the molecular geometrical centers of fluorescein and dabcyl. This distance corresponds to a FRET efficiency of 94.28 % and this distance is within the Forster radius of 46.97 Å.

The theoretical spectrum shows that there is a complete spectral overlap between the absorption and fluorescence spectra responsible for the quenching of the fluorescence due to the FRET effect. Also the fluorescence of fluorescein in the conjugated system 6 TS occurs at wavelength of 432.9 nm, 39.2 nm larger than in the individual molecule due to some energy being lost because of the FRET effect.

The results from this article and the methodology used can help scientists design other MB systems with special significance in molecular diagnosis and in developing DNA sensors.

Acknowledgments SMAG gratefully acknowledges a Doctoral fellowship from Consejo Nacional de Ciencia y Tecnología in Mexico (CONACyT). SMAG, MG, PLA, NFH, and DGM are researchers from the Consejo Nacional de Ciencia y Tecnología in Mexico.

References

1. Tyagi S, Kramer FR (1996) Molecular beacons: probes that fluoresce upon hybridization. Nat Biotechnol 14:303–308. doi:10.1038/nbt0396-303
2. Tyagi S, Bratu DP, Kramer FR (1998) Multicolor molecular beacons for allele discrimination. Nat Biotechnol 16:49–53. doi:10.1038/nbt0198-49
3. Stryer L (1978) Fluorescence energy transfer as a spectroscopic ruler. Annu Rev Biochem 47:819–846. doi:10.1146/annurev.bi.47.070178.004131
4. Förster T (1996) In: Sinanoglu O (ed) Modern quantum chemistry, vol 3. Academic, New York, p 93
5. Kim JH, Morikis D, Ozkan M (2004) Adaptation of inorganic quantum dots for stable molecular beacons. Sensors Actuators B 102:315–319. doi:10.1016/j.snb.2004.04.107

6. Sokol DL, Zhang X, Lu P, Gewirtz AM (1998) Real time detection of DNA·RNA hybridization in living cells. Proc Natl Acad Sci USA 95:11538–11543. doi:10.1073/pnas.95.20.11538
7. Liu X, Farmerie W, Schuster S, Tan W (1999) Molecular beacons for DNA biosensors with micrometer to submicrometer dimensions. Anal Biochem 15:56–63. doi:10.1006/abio.2000.4656
8. Matsuo T (1998) In situ visualization of messenger RNA for basic fibroblast growth factor in living cells. Biochim Biophys Acta 1379:178–184. doi:10.1016/S0304-4165(97)00090-1
9. Alvarado-González M, Crozier PS, Flores-Holguín N, Gallo M, Orrantia-Borunda E, Glossman-Mitnik D (2009) Computational prediction of the melting temperature of a DNA biosensor to detect Mycobacterium tuberculosis. Mol Struct THEOCHEM 912:60–62. doi:10.1016/j.theochem.2009.03.003
10. Li Y, Zhou X, Ye D (2008) Molecular beacons: an optimal multifunctional biological probe. Biochem Biophys Res Commun 373:457–461. doi:10.1016/j.bbrc.2008.05.038
11. Bonnet G, Tyagi S, Libchaber A, Kramer FR (1999) Thermodynamic basis of the enhanced specificity of structured DNA probes. Proc Natl Acad Sci USA 96:6171–6176
12. (Materials Studio 5.5, DMOL^3), http://www.accelrys.com
13. Frisch MJ, Trucks GW, Schlegel HB, Scuseria GE, Robb MA, Cheeseman JR, Montgomery JA Jr, Vreven T, Kudinb KN, Burant JC, Millam JM, Iyengar SS, Tomasi J, Barone V, Mennucci B, Cossi M, Scalmani G, Rega N, Pebterbsson GA, Nakatsuji H, Hada M, Ehara M, Toyota K, Ukuda R, Hasegawa J, Ishida M, Nakajima T, Honda Y, Kitao O, Nakai H, Klene M, Li X, Knox JE, Hratchian HP, Cross JB, Adamo C, Jaramillo J, Gomperts R, Stratmann RE, Yazyev O, Austin AJ, Cammi R, Pomelli C, Ochterski JW, Ayala PY, Morokuma K, Voth GA, Salvador P, Dannenberg JJ, Zakrzewski VG, Dapprich S, Daniels AD, Strain MC, Farkacs O, Malick DK, Rabuck AD, Raghavachari K, Foresman JB, Ortiz JV, Cui Q, Baboul AG, Clifford S, Cioslowski J, Stefanov BB, Liu G, Liashenko A, Piskorz P, Komaromi I, Martin RL, Fox DJ, Keith T, Al-Laham MA, Peng CY, Anayakkara A, Challacombe M, Gill PMW, Johnson B, Chen W, Wong MW, Gonzalez C, Pople JA (2003) Gaussian 03, Revision B.05. Pople. Gaussian Inc, Pittsburgh
14. Adamo C, Barone V (1999) Toward reliable density functional methods without adjustable parameters: the PBE0 model. J Chem Phys 110:6158–6169. doi:10.1063/1.478522
15. Aguilar MA, Olivares del Valle FJ, Tomasi J (1993) Nonequilibrium solvation: an ab-initio quantum–Chemicals method continuum cavity approximation. J Chem Phys 98:7375–7384. doi:10.1063/1.464728
16. Alvarado-González M, Flores-Holguín N, Gallo M, Orrantia-Borunda E, Glossman-Mitnik D (2010) TD-DFT/IEFPCM determination of the absorption and emission spectra of DABCYL. Mol Struct THEOCHEM 945:101–103. doi:10.1016/j.theochem.2010.01.014
17. Grimme S (2006) Semiempirical ggc-type density functional constructed with a long-range dispersion contribution. J Comput Chem 27(15):1787–1799. doi:10.1002/jcc.20495
18. Tkatchenko A, Scheffler M (2009) Accurate molecular van der Waals interactions from ground-state electron density and free-atom reference data. Phys Rev Lett 102:073005. doi:10.1103/PhysRevLett.102.073005
19. Kristyan S, Pulay P (1994) Can (semi)local density functional theories account for the London dispersion forces? Chem Phys Lett 229:175. doi:10.1016/0009-2614(94)01027-7
20. Perez-Jorda JM, Becke AD (1995) A density-functional study of van der Waals forces: rare gas diatomics. Chem Phys Lett 233:134. doi:10.1016/0009-2614(94)01402
21. Zhan CG, Spencer PS, Dixon DA (2004) Chromogenic and neurotoxic effects of an Aliphatic γ-Diketone: computational insights into the molecular structures and mechanism. J Phys Chem B 108:6098–6104. doi:10.1021/jp0312868
22. Gorelsky SI (2009) SWizard Program. University of Ottawa, Ottawa, Canada, Available from http://www.sg-chem.net/. Accessed 11 June 2010
23. May RA, Stevenson KJ (2009) Software Review of Origin 8. J Am Chem Soc 131:2, 872. www.originlab.com/ University of Texas at Austin
24. Spector DL, Goldman RD (2005) Basic methods in microscopy: protocols and concepts from cells: a laboratory manual. Cold Spring Harbor Laboratory Press, 1st edn